LAWRENCE
LIVERMORE
NATIONAL
LABORATORY

LLNL-JRNL-667351

Development and Testing of Diglycolamide Functionalized Mesoporous Silica for Sorption of Trivalent Actinides and Lanthanides

J. Shusterman, H. Mason, J. Bowers, A. Bruchet, E. Uribe, A. B. Kersting, H. Nitsche

February 13, 2015

ACS Applied Materials and Interfaces

Disclaimer

Development and Testing of Diglycolamide Functionalized Mesoporous Silica for Sorption of Trivalent Actinides and Lanthanides

Jennifer Shusterman[†,*], Harris Mason[‡], Jon Bowers[†], Anthony Bruchet[†], Eva Uribe[†], Annie B. Kersting[‡], and Heino Nitsche[†,**]

[†]Department of Chemistry, University of California, Berkeley; Berkeley, California, 94720.

[‡]Glenn T. Seaborg Institute, Physical and Life Sciences Directorate, Lawrence Livermore National Laboratory, L-231, PO Box 808, Livermore, California, 94550.

**Deceased

ABSTRACT

Sequestration of trivalent actinides and lanthanides present in used nuclear fuel and legacy wastes is necessary for appropriate long-term stewardship of these metals particularly to prevent their release into the environment. Organically-modified mesoporous silica is an efficient material for recovery and potential subsequent separation of actinides and lanthanides because of its high surface area, tunable ligand selection, and chemically robust substrate. We have synthesized the first novel hybrid material composed of SBA-15 type mesoporous silica functionalized with diglycolamide ligands (DGA-SBA). Because of the high surface area substrate, the DGA-SBA was found to have highest Eu capacity reported so far in the literature of all DGA solid-phase extractants. The sorption behavior of europium and americium on DGA-SBA in nitric and hydrochloric acid media was tested in batch contact experiments. DGA-SBA was found to have high sorption of Am and Eu at high nitric and hydrochloric acid concentrations, which makes it promising for sequestration of these metals from used nuclear fuel or legacy waste. The kinetics of Eu sorption were found to be two times slower than for Am in 1 M HNO_3, which could aid in subsequent separation of these metals from one another. Additionally, the susceptibility of DGA-SBA to degradation in the presence of acid was probed using ^{29}Si and ^{13}C solid-state NMR spectroscopy. The material was found to be relatively stable in acidic conditions, with the ligand remaining intact after 24 hours of contact with 1 M HNO_3, an important consideration in reuse of the DGA-SBA.

INTRODUCTION

Used nuclear fuel and legacy defense wastes contain significant quantities of trivalent lanthanides and actinides; approximately 10.7 kg of trivalent lanthanides and actinides are present in each ton of used nuclear fuel from pressurized water reactor with typical burnup.[1] The two methods of disposal that are currently being proposed

for this waste are either long-term geologic disposal, or partitioning and transmutation of the trivalent actinides.[1] In either disposal regime, separation of the trivalent minor actinides from the fission product lanthanides and potentially from one another could reduce the volume of waste requiring long-term disposal and reduce costs. The trivalent actinides of interest are curium (Cm) and americium (Am). Americium is of special interest as it exists in larger quantities and has a longer half-life than Cm ($t_{1/2}$ (^{241}Am)= 432.6 y vs. $t_{1/2}$(^{244}Cm)= 18.1 y). Additionally, the dominant ^{241}Am isotope decays to the long lived ^{237}Np ($t_{1/2}$= 2.144 x 10^6 y) and the separation, sequestration and transmutation of Am has the potential to reduce the lifetime of a geologic nuclear waste repository. The early lanthanides exist as both stable and short-lived fission products in much greater quantities than the aforementioned actinides (> 15x more lanthanides than trivalent minor actinides),[1] and complicate separation of the trivalent actinides.[1] Given these challenges new methods must be developed to facilitate these separations.

The minor actinides and the lanthanides exhibit very similar chemistry in acidic media due to their trivalent charge state and nearly identical ionic radii.[2] As a result, separations based on size exclusion or differences in oxidation state are not frequently successful. Because of the electronic structure of the actinides relative to the lanthanides, their bonds are typically found to be more covalent in nature, allowing for separations that exploit these small differences.[3] Replacing the current liquid-liquid extraction methods,[4] with a system based on a solid-phase extractant (SPE) could eliminate the large volumes of hazardous waste generated during separations because of both the lack of organic phase and the potential for reusability. Solid-phase extractants, or extraction chromatography resins, have been synthesized in many different forms and have been made commercially available for the purpose of actinide and lanthanide separations.

An extraction chromatography resin can be produced by coating, impregnation, or covalent bonding of an extractant ligand to a solid support. The method of production greatly impacts the stability of the overall material. Ligand coating is the most common and easiest synthetic route, and allows the use of a wide variety of ligands since no reactive groups on the inert support structure are necessary. The coated particles, however, often demonstrate poor long-term stability since the high acid concentration or radiation dose can cause the

ligands to degrade and to fall off the support structure.[5,6] Additionally, large volumes of solution flushing through the solid-phase or the use of high pressure can reduce the lifetime of the coated SPE materials. Impregnating the ligand traps the ligand in either the solid support matrix itself or in a polymer filling of a porous substrate. This procedure is typically done with silica substrates and has the advantage that the ligand is immobilized in the solid support making it less susceptible to degradation.[7–9] The directionality of the ligand, however, is not easily controlled resulting in a random ordering of ligands on the surface, which may lower the percentage of available ligands for binding with the metal. Due to the limitations of the first two methods, the present work investigates grafting the ligand with a covalent bond to a solid-support in order to add stability and control ligand directionality for improved resins. [10]

The solid-support utilized in this work is SBA-15 type mesoporous (mesoporous defined by 2-50 nm pore diameter) silica. SBA-15 has a well ordered, 2d hexagonal pore structure, with a very high surface area (typically >800 m^2/g).[11] Organically-modified mesoporous silica has been previously synthesized and utilized for lanthanide and actinide sorption utilizing a variety of ligands.[10,12–15] The ligand selected for this work is a diglycolamide (DGA). As diglycolamide ligands are composed of only carbon, hydrogen, oxygen, and nitrogen (CHON), they are completely incinerable at end of use. DGA ligands have been shown to efficiently extract trivalent actinides and lanthanides from highly acidic (> 1 M) nitric acidic feeds in the nuclear fuel cycle using solvent extraction.[16–19] DGA has been made into a resin by coating it on polymer supports, and is now commercially available.[20–23] Some work has been done immobilizing DGA on solid supports via impregnation.[24–26] Recently DGA ligands were covalently bound to silica supports for actinide and lanthanide sorption.[27–29] DGA has been found to form aggregates in high concentrations of nitric acid that have a high affinity the trivalent lanthanides and actinides.[30,31] As Chavan et al discuss,[32] due to this aggregation, preorganization of the DGA on a solid support would result in a more efficient extraction of Am(III) and Eu(III) than achieved with a liquid-liquid system. The current work is aimed at creating more stable materials, with higher ligand density and in turn greater extraction efficiency, by utilizing high surface area mesoporous silica and covalently binding the DGA ligands to the surface.

EXPERIMENTAL METHODS

Material Preparation

Spherical particle SBA-15 type mesoporous silica with 8 nm pore diameter was synthesized based on the procedure from Katiyar et al.[33] The "DGA" ligand was a 4:1 mixture of N,N-(dipropyl)-N'(methyl), N'(3-[trimethoxysilyl]propyl)-3-oxapentane diamide and N,N-(dipropyl)-N'(methyl), N'(3-[monoethoxydimethoxysilyl] propyl)-3-oxapentane diamide (Technocomm) (Figure 1). The DGA ligand was grafted to the silica surface using a solution polymerization technique.[34,35] Condensation of the oxysilanes to the silica surface was conducted under toluene reflux, and then followed by distillation of methanol, water, and a portion of the toluene for volume reduction. The mixture was filtered, washed with 2-propanol, and air-dried overnight. Particles were stored in an evacuated desiccator over time to prevent exposure to moisture.

Characterization

The mesoporous silica was characterized using scanning electron microscopy (SEM), nitrogen adsorption isotherms (BET/BJH method) and infrared spectroscopy (IR). The DGA functionalized mesoporous silica (DGA-SBA) was characterized using infrared spectroscopy, thermogravimetric analysis (TGA), nitrogen adsorption isotherms (BET/BJH method), and nuclear magnetic resonance (NMR) spectroscopy. All parameters and methods associated with these techniques are presented in the supporting information (SI).

Batch Sorption Experiments

Eu(III) stocks were prepared in either pH 3 nitric or hydrochloric acids with a ^{152}Eu tracer. ^{243}Am(III) stock was prepared by purifying the Am(III), boiling it to dryness, and redissolving in either pH 3 nitric or hydrochloric acid. Solid to liquid ratios for all batch experiments were 1 mg solid to 1 mg solution. DGA-SBA solid was pre-equilibrated with the appropriate acid solution (nitric or hydrochloric acid) for 14-17 hrs after pH adjustment. Pre-equilibrated samples were spiked with either Eu(III) or Am(III) stock such that the total metal Eu(III) or Am(III) concentration was approximately 10 μM. Solution pH was monitored and adjusted throughout each experiment. Samples were centrifuged at 5000 rpm for 5 min prior to each aliquot removal. Aliquots were

removed from the supernatant of the samples at approximately 1, 3, and 24 hrs after metal addition for the capacity and pH dependence experiments. For the kinetic experiments, aliquots were removed at several time points ranging between 8 minutes and 9 hours after metal addition. To determine Eu sorption capacity, 5 stock solutions of varying Eu concentrations were prepared, such that a 50 µL addition of the appropriate stock to 6 mL 1 M nitric acid would results in Eu concentrations of 75, 125, 250, 500, and 1000 µM.

Desorption experiments were conducted by first contacting pre-conditioned DGA-SBA with 10 µM Eu or Am in 1 M HNO_3 for 24 h. The samples were centrifuged and aliquots were taken from the supernatant prior to removal from the solids. Two methods of desorption were tested: 1) rinsing with pH 5 HCl and 2) rinsing with ethylenediaminetetraacetic acid (EDTA). For these two methods, the Eu- or Am-contacted DGA-SBA was rinsed multiple times with 1.5 mL of pH 5.5 HCl or 1 mM EDTA, respectively, taking aliquots of each rinse to monitor desorption. During pre-equilibration and between aliquot removal, samples were rocked top-to-bottom.

The concentration of Eu(III) in the aliquots was monitored via the ^{152}Eu tracer using a high-purity germanium (HPGe) gamma spectrometer quantifying based on the 344 keV gamma peak. Am(III) concentration in the aliquots was measured using liquid scintillation counting (LSC) with Ecolume scintillation cocktail. All experiments were conducted in duplicate such that results agreed within 6%. For controls, no-solid blanks were measured which were run in an identical fashion to the batch sorption experiments, but without solid to verify that no precipitation or sorption to the tube was occurring. Additional controls with bare SBA-15 were also run in the same manner as the DGA-SBA batch sorption experiments. These were conducted to measure sorption to the bare silica surface with no ligand present. In both the no-solid blanks and the bare SBA-15 controls, no Am(III) or Eu(III) sorption was observed within uncertainty of the measurement under any conditions examined in this work. Error bars represent 1σ and are based on propagation of pipetting and counting errors.

RESULTS AND DISCUSSION

Material characterization

The SEM micrograph of the silica particles indicates that their average shape is spherical (Figure S1). The BET analysis of the SBA-15 mesoporous silica measures a surface area of 830 m^2/g and an average pore diameter of 7.5 nm. After functionalization, the surface area and pore diameter both decrease to 397 m^2/g and 5.5 nm, respectively. Based on the mass loss measured in the TGA, the ligand density of the DGA-SBA was 0.62 ± 0.03 ligands/nm^2 calculated using a weighted average of the molecular weights of the trimethoxy- and dimethoxymonoethoxysilane attachments on the DGA ligand accounting for the loss of a methoxy- group during grafting. All of the IR spectra contain the characteristic absorption bands for silica at 1070, 965, 805 cm^{-1} corresponding to the symmetric Si-O-Si stretch, the Si-O stretch of surface silanols, and the antisymmetric Si-O-Si stretch, respectively. In comparing the pristine DGA-SBA (Figure S2b) to the non-functionalized SBA (Figure S2a), there is a stretch at 1650 cm^{-1} due to the amide carbonyl stretches of the DGA ligand.

The $^{29}Si\{^1H\}$ CP/MAS NMR spectrum (Figure 2a) of the pristine solid contained six resonances (Table S1); three are associated with the bulk silica material (Q species, δ_{Si} = −92 to −112 ppm) and three with silicon atoms bound to ligands on the surface (T species, δ_{Si} = −50 to −70 ppm). The Q^n species are defined as $Si(OSi)_n(OH)_{4-n}$ and the T^m species are similarly defined as $SiR(OSi)_m(OH)_{3-m}$. For bare, non-functionalized silica, the $^{29}Si\{^1H\}$ CP/MAS spectrum only contains Q peaks, so the presence of T peaks indicates that the ligand was covalently bound to the silica surface. T^1 (δ_{Si} = −51 ppm)[36] peaks are a result of ligand monomers on the surface. T^2 (δ_{Si} = −58 ppm)[36] peaks are from Si atoms bound to terminal ligands in a polymer chain, whereas T^3 (δ_{Si} = −69 ppm)[36] peaks are from the Si atoms bound to central ligands in the polymer chain. From this spectrum, it is clear that all three species are present. Ideally, the material would be primarily composed of T^2 and T^3 species, indicating polymerization of the ligands. Ligand polymerization is important for complexation with the DGA ligand, as 2-3 ligands are necessary to complex Ln(III) and An(III) of interest depending on the specific metal. [18,37] In addition, $^{13}C\{^1H\}$ CP/MAS NMR spectrum was used to determine whether the ligand remained intact during the functionalization process. The spectrum shown in Figure 3a contains six resonances (Table S2), three of which

were used as evidence that the ligand did not decompose during functionalization: δ_C= 167 ppm (C=O), δ_C= 67 ppm (C-O), and δ_C= 6.7 ppm (-CH_3).

Acid hydrolysis

The stability of DGA-SBA was examined by contacting the solid for one day with 1 M HNO_3 to simulate the conditions used for batch sorption experiments to achieve sorption. A $^{29}Si\{^1H\}$ CP/MAS NMR spectrum of the acid-contacted sample (Figure 2b) was collected and compared to the pristine material. While CP is inherently not quantitative, peak ratios of the T peaks can still be compared since the spectra were collected under identical conditions. The T^1:T^2 ratios decreased from 0.86 to 0.34 for the pristine compared to the acid degraded sample, respectively. The T^2:T^3 ratios for the pristine and acid degraded sample were 4.18 and 2.76, respectively. This indicates that the T^2 and T^3 species are not as substantially affected by acid contact as T^1 species, which are substantially hydrolyzed from the surface. This result indicates that ligand polymerization may potentially help stabilize the functionalized materials to acid-catalyzed hydrolysis.

The $^{13}C\{^1H\}$ CP/MAS NMR spectrum of the acid-contacted sample (Figure 3b) shows no substantial difference from the the$^{13}C\{^1H\}$ CP/MAS NMR spectrum of the pristine sample, indicating that after one day of contact with 1 M HNO_3, the ligand does not decompose. While the ^{29}Si NMR spectra indicate cleavage of the isolated ligands on the surface, the polymerized ligands remained grafted, and based on the ^{13}C NMR spectra, it is clear that the ligands remained intact. The IR spectra of the pristine DGA-SBA (Figure S2b) and the acid-contacted DGA-SBA (Figure S2c) are nearly identical, which agrees with the results from the NMR spectroscopy indicating that the ligand remains intact after acid-contact.

Batch sorption

Eu and Am kinetics

The kinetics of Eu and Am sorption to DGA-SBA in 1 M HNO_3 were examined in batch sorption style experiments (Figure 4). The results indicate that Am (Figure 4a) reaches equilibrium after approximately 42 minutes, whereas Eu (Figure 4b) does not reach equilibrium until it has contacted with the solid for approximately 2 hours. The Am and Eu data fit to a pseudo-second-order rate model (Figure S3) with rate constants presented in Table S3.

194 The difference in sorption kinetics could potentially be exploited in a separation of these two species using DGA-
195 SBA as an extraction chromatography material.

196 *Eu and Am sorption in HNO_3 and HCl*
197
198 The equilibrium sorption of Eu(III) and Am(III) by DGA-SBA was studied as a function of nitric and hydrochloric
199 acid concentration. The concentration of nitric and hydrochloric acid was controlled by molarity for the 3 M and
200 1 M samples and by pH adjustments for the pH 1-4 samples. Results of these experiments after ~3 hrs of
201 reaction time are presented in Figure 5. Complete sorption of Eu and Am by DGA-SBA was observed in pH 1, 1
202 M, and 3 M HNO_3 solutions. As discussed previously, equilibrium is reached in less than three hours under the
203 conditions where full sorption occurs, so the sorption data at this time point compared to the 24 hour contact
204 data is the same within error. However, at higher pH values, there is not full sorption of either Am or Eu and the
205 samples do not reach equilibrium within 3 hours. Sorption decreases substantially at higher pH with 60%
206 sorption at pH 2 and 3, and only 40% at pH 4 after 24 hours of contact for Eu. After the same contact time, 78%,
207 51%, and 45% of the Am sorbs to the DGA-SBA at pH 2, 3, and 4, respectively. The corresponding K_d values,
208 however, are still quite high at all nitric acid concentrations tested (Table 1). Those for the highest nitric
209 concentrations (for Eu, 3.2×10^4 and 1.5×10^4 for 1 M and 3 M HNO_3, respectively) agree well with the literature
210 for similar materials.[22,27]

211 The Eu exhibits similar equilibrium sorption behavior in HCl compared to that in HNO_3. A difference in
212 sorption behavior, however, can be observed at 0.01 M acid concentration where 63% ± 6% of the Eu sorbed in
213 HCl relative to 35% ± 4% in HNO_3 at the same concentration. At 0.1 M, 1 M, and 3 M HCl, Eu sorption was
214 identical to sorption from HNO_3, which resulted in nearly complete sorption from a 10 µm Eu solution.
215 Interestingly, Am did not have as high sorption in HCl at concentrations of 0.01 M, 1 M, and 3 M and higher as
216 Eu. At the very high acid concentrations tested, Am sorption never reaches 95-100%, as observed in HNO_3. At
217 0.01 M HCl, Eu has much higher sorption than Am, 63% ± 6% relative to 24% ± 6%, respectively. This difference
218 could be utilized in chromatographic separations. In terms of K_d values, that correlates to 2.8×10^3 (Eu) and $7.4 \times$
219 10^2 (Am) after 24 h of metal-solid contact time, resulting in in a separation factor of Eu to Am of 3.8. Separation

factors at equilibrium derived from batch experiments; however, do not always accurately predict the separations that can be achieved in a chromatographic separation as the solid:liquid ratios and kinetics are significantly different in these two cases and column characteristics must be taken into account.[38] By combining the slightly different behavior in hydrochloric acid especially at shorter contact times, a chromatographic separation of Am from Eu may be possible using DGA-SBA as a solid-phase. Future work will include testing the chromatographic potential of DGA-SBA.

Eu capacity

The capacity of DGA-SBA was determined for Eu(III) in 1 M HNO_3 (Figure S4). Based on the overall similar chemistry of Eu(III) and Am(III) in 1 M HNO_3, we expect that their sorption capacity will be similar under these conditions, and Eu is much less costly than the ^{243}Am required for this measurement. For this experiment, stocks of varying Eu concentrations were added to samples of the same DGA-SBA mass and acid volume and concentration. The capacity was determined from the concentration of Eu measured in the supernatant after 24 hours of contact. Two different adsorption isotherm models, Langmuir (Figure S5) and Freundlich (Figure S6), were used. A linear regression was applied and the sorption data were best described with a Langmuir isotherm. From the Langmuir fit, the capacity of the DGA-SBA for Eu(III) was found to be 379 µmol/g. As with any model, however, it is important to keep in mind the assumptions and limitations. The Langmuir model assumes a smooth surface and monolayer sorption. The Freundlich model, however, better accounts for a more heterogeneous surface. Based on the surface coverage of the ligand determined by TGA and the presence of T^1 species in the $^{29}Si\{^1H\}$ CP/MAS NMR spectrum, there is not a complete monolayer of ligand on the surface. The better fit of the Langmuir model compared to Freundlich may indicate that the Eu is primarily interacting in areas of local well-ordered monolayer formation. The Eu sorption capacities derived from the Langmuir model allowed for the determination of an approximately 2:1 ligand:metal ratio based on the ligand coverage on the surface as measured by TGA. It should be noted that this ratio is a maximum as the ligand coverage measured by TGA is from before contact with acidic solution, which as noted previously, does hydrolyze a portion of the ligands. This agrees with the expected behavior; typically a 3:1 ligand:metal ratio is observed with DGA:Ln

246 complexes in solution. Yet, due to immobilization on a surface, it may more difficult for a third ligand to complex
247 the metal compared to free ligands in a liquid-liquid separation.

248 *Eu and Am desorption*
249
250 The desorption of Eu and Am that was sorbed to DGA-SBA in nitric acid was tested because of its importance in
251 the processing of used nuclear fuel. Eu and Am sorbed to DGA-SBA was expected to effectively desorb in pH 4.5
252 HCl based on the observed trend in percent sorption as a function of pH of HCl. Due to the remaining 1M HNO_3
253 left after decanting the supernatant of the sorption solution, pH 5.5 HCl was used as the rinse solution which
254 resulted in a pH of the third rinse of 4.5. Initially the rinse had a pH of approximately 1.5, which was raised to
255 3.5 with the second rinse, and finally 4.5 with the third rinse. While a final pH of 4.5 was desired, the pH was not
256 adjusted on earlier rinses as this was a desorption method being tested for chromatographic separations. This
257 desorption method was only moderately effective. For Eu, after two rinses with pH 5.5 HCl and 1 day contact,
258 31% of the metal desorbed. Am desorption was similar with 33% Am removal after two rinses. It should be
259 noted, however, that after three rinses, 65% of the Am was desorbed. To determine whether the especially low
260 percent desorption in the first two rinses was due to the pH or nitrate presence, a comparison experiment was
261 conducted where the pH was adjusted with NaOH to 4.5 with each rinse. The Am desorption was not
262 significantly different from that observed with no pH adjustment, which points to a system dominated by nitrate
263 concentration. While batch desorption with this method was not as effective as necessary for a separation
264 (ideally >90% desorption), we expect that this would be much more successful in a chromatography experiment
265 where the nitrate can be more effectively washed from the solid.

266 As expected based on previous work,[27,29] EDTA was effective at completely desorbing Am from the DGA-
267 SBA. While one rinse with 1 mM EDTA only removed 12% of the Am, a second rinse desorbed an additional 82%
268 of the original Am, and third rinse successfully removed the remaining Am. Similarly, desorption of Eu from the
269 DGA-SBA using 1 mM EDTA was tested. The desorption of Eu with EDTA was not quite as successful as it was for
270 Am, with a maximum of 80 % of the Eu being removed after three rinses. The first and second rinses desorbed
271 less than 10% and 75%, respectively. The lower overall desorption of Eu compared to Am may be indicative of a

stronger Eu-DGA complex relative to the Am-DGA complex and agrees with the higher K_d observed for Eu compared to Am in 1 M HNO_3 (Table 1).

Complexation in Eu-DGA-SBA

The complexation of Eu to the DGA-SBA was explored using $^{29}Si\{^1H\}$ and $^{13}C\{^1H\}$CP/MAS NMR spectroscopies (Figures 2c and 3c, respectively). Eu is a strong paramagnet, so in the ^{29}Si and ^{13}C NMR spectra, Si and C nuclei that are near enough to the Eu center will experience the influence of its paramagnetism. This results is exhibited with a change in their chemical shift and relaxation behavior. The Eu-DGA-SBA sample was pre-conditioned with 1M HNO_3 prior to Eu addition and subsequent sorption for a 24 hour time period. The filtered, washed, and dried sample was then studied with NMR spectroscopy. In the $^{13}C\{^1H\}$ CP/MAS NMR spectra of Eu-DGA-SBA compared to p-DGA-SBA (Figures 3c and 3b, respectively), it is clear that the resonances at δ_C= 167, 67, and 47 (marked by asterisks on Figure 3c) have disappeared with the addition of Eu. This is not evidence of the ligand decomposing due to acid, as that would have resulted in these peaks also decreasing in the p-DGA-SBA, but rather a result of the paramagnetic nature of the Eu bound to the ligands. The carbon atoms that are directly bound to the oxygen atoms are most affected as these are the closest to the binding site (carbonyl and ether oxygens). However, even carbon atoms that were more distant from the binding site were impacted by the Eu, indicating that the paramagnetic influence could be extending beyond just a few angstroms.

To verify that the disappearance of the peaks at δ_C= 167, 66, and 46 was not due to Eu-catalyzed ligand breakdown, an IR spectrum of the Eu-DGA-SBA sample was collected. The results of the IR measurement of the Eu-DGA-SBA indicates the carbonyl stretch is still present but shifted to 1630 cm^{-1} (Figure S2d) compared to 1640 cm^{-1} in the acid pre-treated solid (Figure S2c). This shift indicates that the ligand is still present and intact, and that the Eu is coordinating through the carbonyls, as expected.[39] Additionally, the intensity of the symmetric Si-O-Si stretch at 1070 cm^{-1} decreased significantly in the Eu-DGA-SBA sample. This decrease may be indicative of a change in the linearity of the bulk silica.[40] One could imagine that prior to complexation the ligands on the surface can rotate and bend freely. However, with two ligands complexing to a single Eu atom, they lose much

of their original rotational and bending freedom. Restraining the ligands through complexation could result in overall increased rigidity of the surface layers of the bulk silica.

The ^{13}C NMR spectrum clearly confirms that the Eu is binding directly to the ligand. To determine if the Eu is also interacting strongly with the silica surface, a $^{29}Si\{^{1}H\}$ CP/MAS NMR spectrum was collected on the Eu-DGA-SBA (Figure 2c). The ^{29}Si NMR spectrum for the Eu-DGA-SBA still contains both T and Q peaks, and the T peak ratios are quite similar to those observed in the p-DGA-SBA. However, the Q^3:Q^4 ratio changed, which could be a result of Eu altering the CP kinetics of these peaks.[41]

Implications

Previous studies have immobilized diglycolamide ligands on silica, [27–29] but this is the first time these ligands have been covalently bound to mesoporous silica, a much higher surface area substrate. The result of using mesoporous silica is that the material has a higher surface area (397 m^2/g) compared to its analog (180 m^2/g)[27] and in turn a higher metal ion capacity. The Eu(III) capacity determined for the DGA-SBA presented here was 379 µmol/g (57 mg/g) which is four times higher than the higher capacity analogous resin (14 mg/g) presented by Verboom, et al.[27] In comparing Eu sorption from 3M HNO_3 for the DGA-SBA to the analogous resins, the DGA-SBA has a much higher K_d at 2.4 $x10^4$ relative to 2.7 x 10^3 and 5.7 x 10^3 for the two resins made by Verboom et al. The same trend is observed for Am; however, these results are not directly comparable as the metal ion concentrations were significantly higher in this work compared to those in the literature. The higher K_d values are likely due to the higher surface area and ligand density of the DGA-SBA material. In comparison to the commercially available DGA resin,[22] the ligand density for the commercially available material is higher at approximately 0.77 ligands/nm^2 (based on 500 m^2/g surface are [42] of Amberchrom-CG71) which is likely due to a thicker ligand layer in the coated material than is possible with a covalently bound material. Eu sorption, however, for the DGA-SBA is again higher compared to the commercially available resin (379 µmol/g vs. 203 µmol/g). The higher capacity for DGA-SBA despite the lower ligand density supports the hypothesis that the coated solid-phase extractants leave many ligands inaccessible to the metal, whereas covalently bound ligands

are more accessible. DGA-SBA has the highest Eu(III) capacity of all diglycolamide solid-phase extractants thus reported.[22,27]

DGA-SBA sorbed Eu and Am effectively in acid concentrations between 0.1 M and 3 M. The nearly complete sorption of both Am(III) and Eu(III) from nitric and hydrochloric acid at these concentrations is promising for sequestration of these metals with DGA-SBA from dissolved used nuclear fuel or legacy waste. Additionally, the stability of the ligand in the presence of acid indicates that the DGA-SBA could be reused, resulting in less waste production per extraction. While desorption with more dilute HCl was only moderately successful in these batch sorption style experiments, it is expected to be much more effective in chromatographic applications. EDTA was effective in completely desorbing the metals from the DGA-SBA. While it is not ideal to use an organic complexing agent to desorb, especially when trying to eliminate hazardous organic waste production, the overall volume and concentration of EDTA is low relative to a liquid-liquid extraction.

Am was found to have much faster sorption kinetics relative to Eu that follow a pseudo-second order rate law. Additionally, over twice the amount of Eu sorbed to the DGA-SBA relative to Am in 0.01 M HCl. The difference in sorption behavior for Am and Eu at 0.01 M HCl could potentially be utilized for a separation, especially if coupled with the difference in sorption kinetics. If Am and Eu could be separated using DGA-SBA, then it would not only be an effective bulk sorbent for trivalent actinides and lanthanides but could also potentially be used to isolate Am from the lanthanide fission products.

SUPPORTING INFORMATION

Material synthesis and characterization methods, peak information for NMR spectra, kinetic fitting, SEM micrograph, IR spectra, and sorption capacity and isotherms.

ACKNOWLEDGEMENTS

The authors would like to thank Professors A. Katz and Long of the University of California, Berkeley for the TGA and nitrogen adsorption measurements, respectively. The authors would also like to thank Professors Long and Yang of the University of California, Berkeley for use of the SEM and IR instruments. This work was supported by

the National Nuclear Security Administration (NNSA) under the Stewardship Science Academic Alliance Program, award number DE-NA0001978 and by the Subsurface Biogeochemical Research Program of the U.S. Department of Energy's Office of Biological and Environmental Research. This work was performed under the auspices of the U.S. Department of Energy by Lawrence Livermore National Laboratory under Contract DE-AC52-07NA27344. J.S. is supported by a DOE NNSA Stewardship Science Graduate Fellowship under Contract No. DE-FC52-08NA28752. E.C.U is supported by a National Science Foundation Graduate Research Fellowship under Grant No. DGE 1106400.

REFERENCES

(1) Nuclear Energy Agency. *Physics and Safety of Transmutation Systems*; 2006.

(2) Shannon, R. D. Revised Effective Ionic Radii and Systematic Studies of Interatomie Distances in Halides and Chaleogenides Central Research and Development Department , Experimental Station , E . L Du Pont de Nemours The Effective Ionic Radii of Shannon & Prewitt [Acta. *Acta Crystallogr.* **1976**, *A32*, 751.

(3) Jensen, M. P.; Bond, A. H. Comparison of Covalency in the Complexes of Trivalent Actinide and Lanthanide Cations. *J. Am. Ceram. Soc.* **2002**, *124*, 9870–9877.

(4) Lewis, F.; Hudson, M.; Harwood, L. Development of Highly Selective Ligands for Separations of Actinides from Lanthanides in the Nuclear Fuel Cycle. *Synlett* **2011**, *2011*, 2609–2632.

(5) Panja, S.; Mohapatra, P. K.; Misra, S. K.; Tripathi, S. C. Carrier Facilitated Transport of Europium(III) Across Supported Liquid Membranes Containing N,N,N □, N □-Tetra-2-Ethylhexyl-3-Oxapentane-Diamide (T2EHDGA) as the Extractant. *Sep. Sci. Technol.* **2011**, *46*, 1941–1949.

(6) Klug, C.; Sudowe, R. A Novel Extraction Chromatography Resin for Trivalent Actinides Using 2,6-bis(5,6-Diisobutyl-1,2,4-Triazine-3-Yl)pyridine. *Sep. Sci. Technol.* **2013**, *48*, 2567–2575.

(7) Hoshi, H.; Wei, Y.-Z.; Kumagai, M.; Asakura, T.; Morita, Y. Separation of Trivalent Actinides from Lanthanides by Using R-BTP Resins and Stability of R-BTP Resin. *J. Alloys Compd.* **2006**, *408-412*, 1274–1277.

(8) Liu, R.; Wang, X.; Wei, Y.; Shi, W.; Chai, Z. Evaluation Study on a Macroporous Silica-Based Isohexyl-BTP Adsorbent for Minor Actinides Separation from Nitric Acid Medium. *Radiochim. Acta* **2014**, *102*, 93–100.

(9) Wei, Y.; Kumagai, M.; Takashima, Y.; Modolo, G.; Odoj, R. Studies on the Separation of Minor Actinides from High-Level Wastes by Extraction Chromatography Using Novel Silica-Based Extraction Resins. *Nucl. Technol.* **2000**, *132*, 413–423.

(10) Fryxell, G. E.; Mattigod, S. V.; Lin, Y.; Wu, H.; Fiskum, S.; Parker, K.; Zheng, F.; Yantasee, W.; Zemanian, T. S.; Addleman, R. S.; et al. Design and Synthesis of Self-Assembled Monolayers on Mesoporous Supports

(SAMMS): The Importance of Ligand Posture in Functional Nanomaterials. *J. Mater. Chem.* **2007**, *17*, 2863.

(11) Zhao, D., Feng, J., Huo, Q., Melosh, N., Fredrickson, G.H., Chmelka, B.F., Stucky, G. D. Triblock Copolymer Syntheses of Mesoporous Silica with Periodic 50 to 300 Angstrom Pores. *Science (80-.).* **1998**, *279*, 548–552.

(12) Bourg, S.; Broudic, J.-C.; Conocar, O.; Moreau, J. J. E.; Meyer, D.; Wong Chi Man, M. Tailoring of Organically Modified Silicas for the Solid−Liquid Extraction of Actinides. *Chem. Mater.* **2001**, *13*, 491–499.

(13) Fryxell, G. E.; Lin, Y.; Fiskum, S.; Birnbaum, J. C.; Wu, H.; Kemner, K.; Kelly, S. Actinide Sequestration Using Self-Assembled Monolayers on Mesoporous Supports. *Environ. Sci. Technol.* **2005**, *39*, 1324–1331.

(14) Fryxell, G. E.; Wu, H.; Lin, Y.; Shaw, W. J.; Birnbaum, J. C.; Linehan, J. C.; Nie, Z.; Kemner, K.; Kelly, S. Lanthanide Selective Sorbents: Self-Assembled Monolayers on Mesoporous Supports (SAMMS). *J. Mater. Chem.* **2004**, *14*, 3356.

(15) Zhang, W.; He, X.; Ye, G.; Yi, R.; Chen, J. Americium(III) Capture Using Phosphonic Acid-Functionalized Silicas with Different Mesoporous Morphologies: Adsorption Behavior Study and Mechanism Investigation by EXAFS/XPS. *Environ. Sci. Technol.* **2014**, *48*, 6874–6881.

(16) Sasaki, Y., Tachimori, S. Extraction of Actinides(III), (IV), (V), (VI), and Lanthanides(III) by Structurally Tailored Diamides. *Solvent Extr. Ion Exch.* **2002**, *20*, 21–34.

(17) Suzuki, B. H.; Sasaki, Y.; Sugo, Y.; Apichaibukol, A.; Kimura, T. Extraction and Separation of Am (III) and Sr (II) by N , N , N , N -Tetraoctyl-3-Oxapentanediamide (TODGA). *Radiochim. Acta* **2004**, *92*, 463–466.

(18) Sasaki, Y.; Sugo, Y.; Suzuki, S.; Tachimori, S. The Novel Extractants, Diglycolamides, for the Extraction of Lanthanides and Actinides in HNO3-N-Dodecane System. *Solvent Extr. Ion Exch.* **2001**, *19*, 91–103.

(19) Kimura, T.; Choppin, G. Luminescence Study on Determination of the Hydration Number of Cm(III). *J. Alloys Compd.* **1994**, *213-214*, 313–317.

(20) Ansari, S. a; Pathak, P. N.; Husain, M.; Prasad, a K.; Parmar, V. S.; Manchanda, V. K. Extraction Chromatographic Studies of Metal Ions Using N,N,N',N'-Tetraoctyl Diglycolamide as the Stationary Phase. *Talanta* **2006**, *68*, 1273–1280.

(21) Husain, M.; Ansari, S.; Mohapatra, P.; Gupta, R.; Parmar, V.; Manchanda, V. Extraction Chromatography of Lanthanides Using N,N,N′,N′-Tetraoctyl Diglycolamide (TODGA) as the Stationary Phase. *Desalination* **2008**, *229*, 294–301.

(22) Horwitz, E. P.; McAlister, D. R.; Bond, A. H.; Barrans Jr., R. E. Novel Extraction of Chromatographic Resins Based on Tetraalkyldiglycolamides: Characterization and Potential Applications. *Solvent Extr. Ion Exch.* **2005**, *23*, 319–344.

(23) Gharibyan, N.; Dailey, A.; McLain, D. R.; Bond, E. M.; Moody, W. a.; Happel, S.; Sudowe, R. Extraction Behavior of Americium and Curium on Selected Extraction Chromatography Resins from Pure Acidic Matrices. *Solvent Extr. Ion Exch.* **2014**, *32*, 391–407.

(24) Modolo, G.; Asp, H.; Schreinemachers, C.; Vijgen, H. Recovery of Actinides and Lanthanides from High-Level Liquid Waste by Extraction Chromatography Using TODGA+TBP Impregnated Resins. *Radiochim. Acta* **2007**, *95*, 391–397.

(25) Zhang, A.; Mei, C.; Wei, Y.; Kumagai, M. Preparation of a Novel Macroporous Silica-Based Diglycolamide Derivative-Impregnated Polymeric Composite and Its Adsorption Mechanism for Rare Earth Metal Ions. *Adsorpt. Sci. Technol.* **2007**, *25*, 257–272.

(26) Van Hecke, K.; Modolo, G. Separation of Actinides from Low Level Liquid Wastes (LLLW) by Extraction Chromatography Using Novel DMDOHEMA and TODGA Impregnated Resins. *J. Radioanal. Nucl. Chem.* **2004**, *261*, 269–275.

(27) Ansari, S. a; Mohapatra, P. K.; Iqbal, M.; Huskens, J.; Verboom, W. Two Novel Extraction Chromatography Resins Containing Multiple Diglycolamide-Functionalized Ligands: Preparation, Characterization and Actinide Uptake Properties. *J. Chromatogr. A* **2014**, *1334*, 79–86.

(28) Mohapatra, P. K.; Ansari, S. a.; Iqbal, M.; Huskens, J.; Verboom, W. First Example of Diglycolamide-Grafted Resins: Synthesis, Characterization, and Actinide Uptake Studies. *RSC Adv.* **2014**, *4*, 10412.

(29) Ansari, S. A.; Mohapatra, P. K.; Iqbal, M.; Huskens, J.; Verboom, W. Sorption of americium(III) and europium(III) from Nitric Acid Solutions by a Novel Diglycolamide-Grafted Silica-Based Resins: Part 2. Sorption Isotherms, Column and Radiolytic Stability Studies. *Radiochim. Acta* **2014**, *102*, 903–910.

(30) Jensen, M. P.; Yaita, T.; Chiarizia, R. Reverse-Micelle Formation in the Partitioning of Trivalent F-Element Cations by Biphasic Systems Containing a Tetraalkyldiglycolamide. *Langmuir* **2007**, *23*, 4765–4774.

(31) Yaita, T.; Herlinger, a. W.; Thiyagarajan, P.; Jensen, M. P. Influence of Extractant Aggregation on the Extraction of Trivalent F-Element Cations by a Tetraalkyldiglycolamide. *Solvent Extr. Ion Exch.* **2004**, *22*, 553–571.

(32) Chavan, V.; Thekkethil, V.; Pandey, A. K.; Iqbal, M.; Huskens, J.; Singh, S.; Goswami, A.; Verboom, W. Assembled Diglycolamide for F-Element Ions Sequestration at High Acidity. *React. Funct. Polym.* **2014**, *74*, 52–57.

(33) Katiyar, A.; Yadav, S.; Smirniotis, P. G.; Pinto, N. G. Synthesis of Ordered Large Pore SBA-15 Spherical Particles for Adsorption of Biomolecules. *J. Chromatogr. A* **2006**, *1122*, 13–20.

(34) Fryxell, G. E.; Liu, J. Designing Surface Chemistry in Mesoporous Silica. In *Adsorption on Silica Surfaces*; Papirer, E., Ed.; 2000; pp. 665–687.

(35) Feng, X., Fryxell, G.E., Wang, L.-Q., Kim, A.Y., Liu, J., Kemner, K. M. Functionalized Monolayers on Ordered Mesoporous Supports. *Science (80-.).* **1997**, *276*, 923–926.

(36) Bibent, N.; Charpentier, T.; Devautour-Vinot, S.; Mehdi, A.; Gaveau, P.; Henn, F.; Silly, G. Solid-State NMR Spectroscopic Studies of Propylphosphonic Acid Functionalized SBA-15 Mesoporous Silica: Characterization of Hydrogen-Bonding Interactions. *Eur. J. Inorg. Chem.* **2013**, 2350–2361.

(37) Antonio, M. R.; McAlister, D. R.; Horwitz, E. P. An Europium(iii) Diglycolamide Complex: Insights into the Coordination Chemistry of Lanthanides in Solvent Extraction. *Dalton Trans.* **2014**, 4–6.

(38) Gharibyan, N. Intragroup Separation of Trivalent Lanthanides and Actinides for Neutron Capture Experiments in Stockpile Stewardship Sciences, University of Nevada, Las Vegas, 2011, p. 196.

(39) Zhang, Y.-L.; Liu, W.-S.; Dou, W.; Qin, W.-W. Synthesis and Infrared and Fluorescence Spectra of New Europium and Terbium Polynuclear Complexes with an Amide-Based 1,10-Phenanthroline Derivative. *Spectrochim. acta. Part A* **2004**, *60*, 1707–1711.

(40) Ohishi, T. Preparation and Properties of SiO2 Thin Films by the Sol-Gel Method Using Photoirradiation and Its Application to Surface Coating for Display. In *Chemical Processing of Ceramics*; 2005; pp. 425–428.

(41) Mason, H. E.; Harley, S. J.; Maxwell, R. S.; Carroll, S. A. Probing the Surface Structure of Divalent Transition Metals Using Surface Specific Solid-State NMR Spectroscopy. *Environ. Sci. Technol.* **2012**, *46*, 2806–2812.

(42) Rohm and Haas. *AMBERCHROM ™ Chromatographic Resins*; 2005; p. 2.

Tables

Cation	Acid	Acid concentration	pH	K_d [mL/g]
Eu(III)	HNO_3	3 M		1.52×10^4
		1 M		3.17×10^4
			0.98	2.17×10^5
			1.98	1.52×10^3
			2.97	1.79×10^3
			3.95	6.36×10^2
	HCl	3 M		1.41×10^4
		1 M		2.45×10^4
			0.98	8.12×10^4
			2.00	2.84×10^3
			3.04	2.13×10^2
			4.01	2.10×10^2
Am(III)	HNO_3	3 M		1.19×10^4
		1 M		1.31×10^4
			1.10	1.67×10^4
			2.06	3.41×10^3
			3.08	1.01×10^3
			3.96	7.68×10^2
	HCl	3 M		7.33×10^3
		1 M		7.74×10^3
			1.10	5.39×10^3
			2.04	7.37×10^2
			3.08	4.64×10^2
			3.99	5.92×10^2

Table 1. Batch sorption results of Eu(III) and Am(III) on DGA-SBA after 24 hours of metal contact time in HNO_3 and HCl. Metal ion concentrations were 8 µM and 10 µM for Am(III) and Eu(III), respectively.

FIGURES

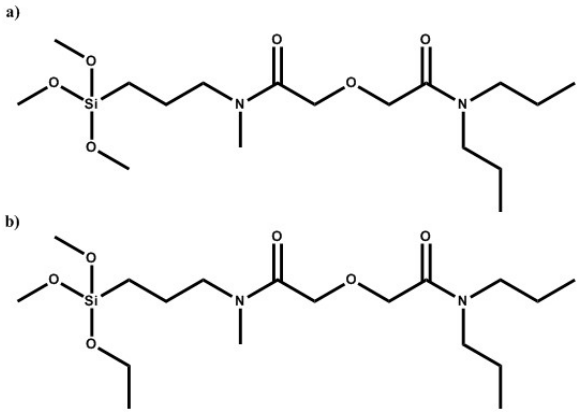

Figure 1. a) N,N-(dipropyl)-N'(methyl), N'(3-[trimethoxysilyl]propyl)-3-oxapentane diamide and b) N,N-(dipropyl)-N'(methyl), N'(3-[monoethoxydimethoxysilyl] propyl)-3-oxapentane diamide. The 'DGA' mixture used in the synthesis was a 4 to 1 ratio of a to b.

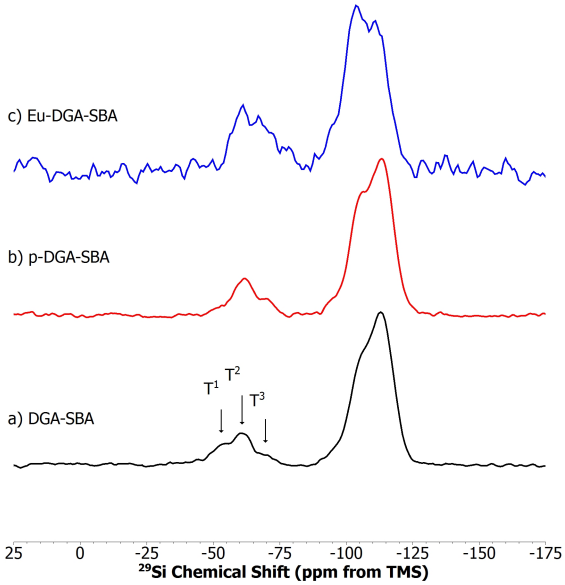

Figure 2. $^{29}Si\{^{1}H\}$ CP/MAS NMR spectra for DGA functionalized SBA-15 a) pristine solid (DGA-SBA), b) acid-contacted solid (p-DGA-SBA), and c) Eu-contacted solid (Eu-DGA-SBA) The resonances for the bulk silicon atoms are the Q peaks (Q^2, Q^3, and Q^4 have shifts of δ_{Si} =-94, -104, and -112 ppm, respectively) and for the surface silicon atoms are the T peaks (T^1, T^2, and T^3 have shifts of δ_{Si} =-54, -60, and -69 ppm, respectively).

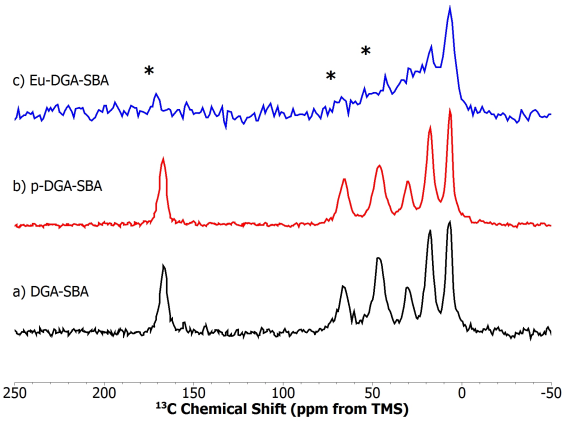

Figure 3. $^{13}C\{^{1}H\}$ CP/MAS NMR spectra for DGA functionalized SBA-15 a) pristine solid (DGA-SBA), b) acid-contacted solid (p-DGA-SBA), and c) Eu-contacted solid (Eu-DGA-SBA) . Asterisks indicate chemical shift of resonances impacted by the presence of Eu.

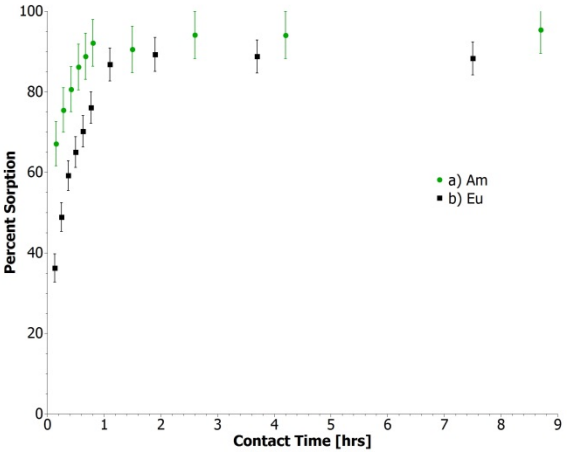

Figure 4. Batch sorption kinetics for a) Am(III) and b) Eu(III) from 1 M nitric acid by DGA-SBA. Eu(III) and Am(III) concentrations were 10 and 8 µM, respectively.

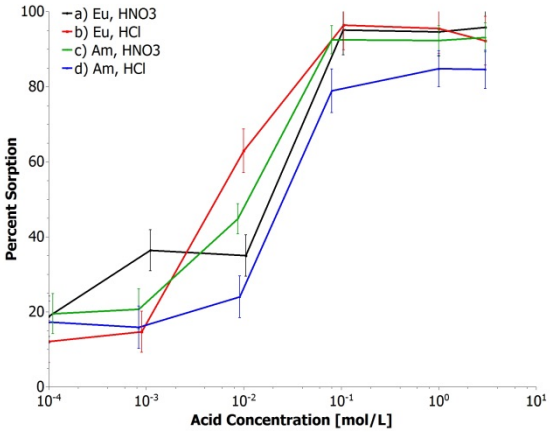

Figure 5. Batch sorption of a, b) Eu(III) and c, d) Am(III) from varying concentrations of nitric and hydrochloric acids by DGA-SBA. Metal-solid contact time was approximately 3 h. Eu(III) and Am(III) concentrations were 10 and 8 µM, respectively.

517 For Table of Contents Only:

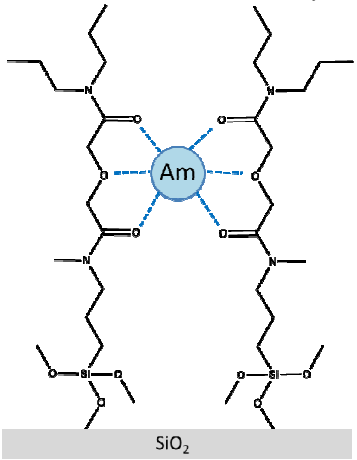

518
519